Weakly Nonlinear Response of a Stably Stratified Atmosphere to Diabatic Forcing in a Uniform Flow

HYE-YEONG CHUN

Atmospheric and Environmental Research Institute and Department of Atmospheric Sciences, Seoul National University, Seoul, Korea

JONG-JIN BAIK

Global Environment Laboratory and Department of Astronomy and Atmospheric Sciences, Yonsei University, Seoul, Korea

(Manuscript received 10 June 1993, in final form 10 February 1994)

ABSTRACT

The weakly nonlinear response of a two-dimensional stably stratified atmosphere to prescribed diabatic heating in a uniform flow is investigated analytically using perturbation expansion in a small value of the nonlinearity factor for the thermally induced waves. The diabatic heating is assumed to have only a zeroth-order term specified to be vertically homogeneous between the surface and a certain height and bell shaped in the horizontal. The first-order (weakly nonlinear) solutions are obtained using the FFT algorithm after solutions in wavenumber space are obtained analytically. The forcing (F) to the first-order perturbation equation induced by the Jacobian of the zeroth-order (linear) solutions always represents cooling in the lower layer regardless of specified forcing type (cooling or heating). The vertical structure of F is related to the nondimensional heating depth (d) or the inverse Froude number. The first-order solutions are valid for relatively small values (<3) of d. The main nonlinear effect is to produce a strong convergence region near the surface associated with the zeroth-order perturbations regardless of the value of d. This convergence is responsible for producing upward motion in the center of the forcing region that extends upstream. As a result, the zeroth-order downward motion becomes weaker according to a degree of nonlinearity. The relative magnitude of the zeroth-order downward motion and the first-order upward motion upstream of the forcing can be determined by d. The source of the first-order wave energy is found to come mainly from the horizontal advection of the zeroth-order total wave energy by the first-order perturbation horizontal wind.

1. Introduction

The theoretical aspects of the circulations induced by localized diabatic forcing in a stably stratified flow have been studied extensively during the past decade because of a wide range of applications to mesoscale meteorology. These include the land/sea breeze, heat islands, orographic–convective rain, rain-induced cold pools in convective systems, etc. Recently, Lin and Stewart (1991) reviewed diabatically forced mesoscale circulations.

In linear analytic studies (e.g., Smith and Lin 1982; Lin and Smith 1986; Raymond 1986; Lin 1987; Bretherton 1988; Lin and Chun 1991; Baik 1992), the localized diabatic forcing is represented by a specified heat source or sink. Some of the noticeable results obtained from the studies mentioned above can be summarized as follows: (i) if the horizontally integrated heating or cooling is nonzero in the inviscid flow system, the two-dimensional steady-state solution exhibits a singularity problem; (ii) there is a negative phase relationship between the heating and the induced vertical displacement by the mean wind advection in both the steady-state and time-dependent cases in a large Froude number flow; (iii) the magnitude of the perturbation in a uniform ambient flow is determined by the thermal Froude number; and (iv) when the basic flow has a constant shear with a critical level, the relationship between the heating specified below the critical level and the induced vertical velocity can be positive or negative depending on the Richardson number of the basic flow and the heating depth, while the vertical motion in the heating center is almost upward for a wide range of the Richardson numbers when the critical level is located in the heating region.

Even though the above studies have contributed to understanding the basic dynamics of the thermally induced circulations, those are constrained by the linear assumption. In the mountain wave problem, there have been several nonlinear analytical studies (e.g., Long 1953; Barcilon and Fitzjarrald 1985; Smith 1985; Smith and Sun 1987). Those investigations of the nonlinear mountain wave problem are possible due to the

Corresponding author address: Dr. Hye-Yeong Chun, Dept. of Atmospheric Sciences, Seoul National University, Seoul 151-742, Korea.

famous equation derived by Long (1953). For uniform ambient wind and constant Brunt–Väisälä frequency in a two-dimensional frame, the nonlinear governing equations are reduced to a single linear equation (Long's equation). Smith (1985) imposed a nonlinear upper-boundary condition on Long's equation and found a condition for possible wave resonance that is a function of the mountain height. His study is a generalization of the linear theory by Peltier and Clark (1983).

However, there is, to the authors' knowledge, no proper nonlinear analytical study on thermally induced waves. This may be because the diabatic forcing term makes nonlinear governing equations difficult to combine into a single linear equation such as Long's equation. One possible way to resolve this problem is to include diabatic forcing as a lower-boundary condition, which is similar to what Lin (1990) did in a study of coastal cyclogenesis. However, in the nonlinear case, the relationship between the buoyancy and the streamfunction at the surface makes the problem much more difficult to solve compared with the nonlinear mountain wave problem. In addition, even if the diabatic forcing represents, for example, a heat island or the differential heating associated with the temperature contrast between land and sea, the depth of the isolated heat source or sink is still finite in nature. Especially when the thermal forcing represents the latent heating due to cumulus convection, the heating depth can be as high as the height of tropopause. Another possible way to overcome the problem is to assume that the diabatic forcing is proportional to the vertical velocity in each layer. In this case, the diabatic forcing term can be combined with the buoyancy term in terms of the vertical velocity. This, however, reduces the forced problem to an eigenvalue problem.

There have been several theoretical studies of two-dimensional nonlinear stratified flow with applications to the processes of organized convection primarily by one group—namely, Moncrieff and Green (1972), Moncrieff and Miller (1976), Moncrieff (1978), Thorpe et al. (1980), and Moncrieff (1981). In their models, they assumed that the flow is steady state, inviscid, and, especially, that the diabatic forcing is proportional to the vertical velocity and the lapse rate specified by the inflow level necessary to obtain the conservative variables. Therefore, the physical problem becomes an eigenvalue problem with imposed rigid upper and lower boundaries. In the eigenvalue problem, the heating can modify gravity waves, but cannot generate them (Smith and Lin 1982). Therefore, at this point a weakly nonlinear approach seems to be one feasible way to analytically investigate the nonlinear response of a stably stratified flow to prescribed thermal forcing.

Lin and Chun (1991) first introduced a nonlinearity parameter (μ) for the thermally induced internal waves. Baik (1992) applied this nonlinearity parameter to the heat island problem using a two-dimensional numerical model and showed that for small values of μ the response resembles the linear steady-state solution, while for large values of μ the behavior is quite different from that predicted by the linear solution.

In this paper, we solve a weakly nonlinear problem through perturbation expansion in a small value of the nonlinearity parameter in order to investigate the nonlinear response to prescribed thermal forcing. In section 2, the governing equations and solutions to the zeroth-order and the first-order equations are given. In section 3, the energy equation is derived and discussed. In section 4, the results of the weakly nonlinear response of a stably stratified atmosphere to diabatic forcing are presented and discussed. Finally, a summary and conclusions are given in section 5.

2. Governing equations and solutions

a. Governing equations

Consider a two-dimensional, steady-state, incompressible, hydrostatic, nonrotating, inviscid, Boussinesq airflow system. The equations governing finite-amplitude perturbations in a uniform basic-state horizontal flow with diabatic forcing can be written as

$$U\frac{\partial u}{\partial x} + u\frac{\partial u}{\partial x} + w\frac{\partial u}{\partial z} = -\frac{\partial \pi}{\partial x}, \qquad (1)$$

$$\frac{\partial \pi}{\partial z} = b, \qquad (2)$$

$$U\frac{\partial b}{\partial x} + u\frac{\partial b}{\partial x} + w\frac{\partial b}{\partial z} + N^2 w = \frac{g}{c_p T_0} q, \qquad (3)$$

$$\frac{\partial u}{\partial x} + \frac{\partial w}{\partial z} = 0. \qquad (4)$$

Here x is the horizontal coordinate, z the vertical coordinate, u the perturbation velocity in the x direction, w the perturbation velocity in the z direction, π the perturbation kinematic pressure ($=p/\rho_0$, where p is the perturbation pressure and ρ_0 the basic-state density), b the perturbation buoyancy ($=g\theta/\theta_0$, where g is the gravitational acceleration, θ the perturbation potential temperature, and θ_0 the reference potential temperature), U the uniform basic-state wind in the x direction ($U > 0$), T_0 the basic-state temperature, N the Brunt–Väisälä frequency, c_p the specific heat capacity of air at constant pressure, and q the diabatic forcing function. Equations (1)–(4) are the horizontal momentum equation in the x direction, the hydrostatic equation, the thermodynamic energy equation, and the mass continuity equation, respectively. In this study, the diabatic forcing function is specified as

$$q(x, z) = \begin{cases} q_0 f(x) & \text{for} \quad 0 \leq z \leq d \\ 0 & \text{for} \quad z > d, \end{cases} \qquad (5)$$

$$f(x) = \frac{a_1^2}{x^2 + a_1^2} - \frac{a_1 a_2}{x^2 + a_2^2}, \tag{6}$$

where q_0 is the amplitude of the diabatic forcing function and a_1 (half-width of the bell-shaped function) and a_2 are constants with $a_1 < a_2$. The widespread cooling term [second term on the right-hand side of (6)] is necessary to avoid the net heating or cooling problem in a steady-state, inviscid flow system (Smith and Lin 1982). We define a perturbation streamfunction φ that satisfies $\partial\varphi/\partial x = -w$ and $\partial\varphi/\partial z = u$. Equations (1)–(4) can be combined to yield two equations in the dependent variables φ and b:

$$U\frac{\partial^3\varphi}{\partial x\partial z^2} + \frac{\partial b}{\partial x} - J\left(\varphi, \frac{\partial^2\varphi}{\partial z^2}\right) = 0, \tag{7}$$

$$U\frac{\partial b}{\partial x} - N^2\frac{\partial\varphi}{\partial x} - J(\varphi, b) = \frac{g}{c_pT_0}q, \tag{8}$$

where the symbol J denotes the Jacobian defined by $J(A, B) = (\partial A/\partial x)(\partial B/\partial z) - (\partial A/\partial z)(\partial B/\partial x)$.

As suggested by Lin and Chun (1991), the following nondimensional variables are introduced:

$$x = l\hat{x}, \quad a_1 = l\hat{a}_1, \quad a_2 = l\hat{a}_2,$$

$$z = \left(\frac{U}{N}\right)\hat{z}, \quad d = \left(\frac{U}{N}\right)\hat{d},$$

$$\varphi = \left(\frac{gq_0l}{c_pT_0N^2}\right)\hat{\varphi}, \quad b = \left(\frac{gq_0l}{c_pT_0U}\right)\hat{b}, \quad q = q_0\hat{q}, \tag{9}$$

where l is the horizontal length scale of the diabatic forcing and the caret denotes nondimensional variables. Note that $\hat{d}$ is equal to the inverse of the Froude number associated with the diabatic forcing [Fr $= U/(Nd)$] (Lin and Smith 1986) and therefore may be called the nondimensional heating depth. Substituting the above nondimensional variables into (7), (8), (5), and (6) yields (with all the carets dropped hereafter)

$$\frac{\partial^3\varphi}{\partial x\partial z^2} + \frac{\partial b}{\partial x} - \mu J\left(\varphi, \frac{\partial^2\varphi}{\partial z^2}\right) = 0, \tag{10}$$

$$\frac{\partial b}{\partial x} - \frac{\partial\varphi}{\partial x} - \mu J(\varphi, b) = q, \tag{11}$$

$$\mu = \frac{gq_0l}{c_pT_0NU^2}, \tag{12}$$

$$q(x, z) = \begin{cases} f(x) & \text{for} \quad 0 \leq z \leq d \\ 0 & \text{for} \quad z > d, \end{cases} \tag{13}$$

$$f(x) = \frac{a_1^2}{x^2 + a_1^2} - \frac{a_1 a_2}{x^2 + a_2^2}. \tag{14}$$

It should be noted that the variables in (6) are in the dimensional form, while the variables in (14) are in the nondimensional form. The nonlinearity factor μ for the thermally induced finite-amplitude waves in (12) can be interpreted as a scale ratio of the perturbation horizontal velocity to the basic-state wind (Lin and Chun 1991). Equation (12) indicates that the amplitude of the thermally induced wave is proportional to the amplitude and horizontal length scale of the diabatic forcing and inversely proportional to the basic-state temperature, the Brunt–Väisälä frequency, and square of the basic-state wind speed. This expression was first derived by Lin and Chun (1991) in their study on the effects of diabatic cooling in a stratified shear flow with a critical level, and subsequently applied by Baik (1992) to explain some dynamical aspects of precipitation enhancement observed on the downstream side of the heat islands.

The perturbation streamfunction and buoyancy are expanded in small values of the parameter μ:

$$\varphi = \varphi_0 + \mu\varphi_1 + \mu^2\varphi_2 + \cdots, \tag{15}$$

$$b = b_0 + \mu b_1 + \mu^2 b_2 + \cdots. \tag{16}$$

After substituting (15) and (16) into (10) and (11) and collecting like powers of μ assuming that the diabatic forcing function has only a zeroth-order term (i.e., $q = q_0$) one can obtain the following zeroth-order equations:

$$\frac{\partial^3\varphi_0}{\partial x\partial z^2} + \frac{\partial b_0}{\partial x} = 0, \tag{17}$$

$$\frac{\partial b_0}{\partial x} - \frac{\partial\varphi_0}{\partial x} = q_0, \tag{18}$$

and first-order equations

$$\frac{\partial^3\varphi_1}{\partial x\partial z^2} + \frac{\partial b_1}{\partial x} - J\left(\varphi_0, \frac{\partial^2\varphi_0}{\partial z^2}\right) = 0, \tag{19}$$

$$\frac{\partial b_1}{\partial x} - \frac{\partial\varphi_1}{\partial x} - J(\varphi_0, b_0) = 0. \tag{20}$$

Subtracting (18) from (17) and using the relation $\partial\varphi_0/\partial x = -w_0$ gives

$$\frac{\partial^2 w_0}{\partial z^2} + w_0 = q_0. \tag{21}$$

Similarly, subtracting (20) from (19) and using the relation $\partial\varphi_1/\partial x = -w_1$ gives

$$\frac{\partial^2 w_1}{\partial z^2} + w_1 = F(x, z), \tag{22}$$

where

$$F(x, z) = -J\left(\varphi_0, \frac{\partial^2\varphi_0}{\partial z^2} - b_0\right). \tag{23}$$

We define a one-sided complex Fourier transform pair for any dependent variable by the integral

$$\tilde{G}(k, z) = \frac{1}{\pi}\int_{-\infty}^{\infty} G(x, z)e^{-ikx}dx, \quad (24a)$$

$$G(x, z) = \mathrm{Re}\left\{\int_0^{\infty} \tilde{G}(k, z)e^{ikx}dk\right\}. \quad (24b)$$

b. Zeroth-order (linear) solutions

Taking the Fourier transform of (21) yields

$$\frac{\partial^2 \tilde{w}_0}{\partial z^2} + \tilde{w}_0 = \tilde{q}_0, \quad (25)$$

where for $0 \leqslant z \leqslant d$, $\tilde{q}_0 = a_1(e^{-a_1 k} - e^{-a_2 k})$ and for $z > d$, $\tilde{q}_0 = 0$. The general solution to (25) is

$$\tilde{w}_0(k, z) = A_0(k)e^{iz} + B_0(k)e^{-iz} + \tilde{q}_0 \quad \text{for} \quad 0 \leqslant z \leqslant d, \quad (26a)$$

$$\tilde{w}_0(k, z) = C_0(k)e^{iz} + D_0(k)e^{-iz} \quad \text{for} \quad z > d. \quad (26b)$$

The four coefficients $A_0(k)$, $B_0(k)$, $C_0(k)$, and $D_0(k)$ can be determined by imposing the lower boundary condition of $\tilde{w}_0 = 0$ at $z = 0$; the upper radiation condition (Booker and Bretherton 1967), which requires $D_0(k) = 0$; and the interface conditions that $\tilde{w}_0$ and $\partial\tilde{w}_0/\partial z$ are continuous at $z = d$. Then, it follows that

$$\tilde{w}_0(k, z) = \tilde{q}_0[i(e^{id} - 2)\sin z + 1 - e^{-iz}] \quad \text{for} \quad 0 \leqslant z \leqslant d, \quad (27a)$$

$$\tilde{w}_0(k, z) = -(1 - \cos d)\tilde{q}_0 e^{iz} \quad \text{for} \quad z > d. \quad (27b)$$

The solution for the zeroth-order vertical velocity w_0 field is obtained after taking the inverse Fourier transform of (27a) and (27b) and is found to be

$$w_0(x, z) = X_1(1 - \sin d \sin z - \cos z) + (1 - \cos d)X_2 \sin z \quad \text{for} \quad 0 \leqslant z \leqslant d, \quad (28a)$$

$$w_0(x, z) = -(1 - \cos d)(X_1 \cos z - X_2 \sin z) \quad \text{for} \quad z > d, \quad (28b)$$

where

$$X_1 = \frac{a_1^2}{x^2 + a_1^2} - \frac{a_1 a_2}{x^2 + a_2^2},$$

$$X_2 = \frac{a_1 x}{x^2 + a_1^2} - \frac{a_1 x}{x^2 + a_2^2}.$$

Integration of $\partial\varphi_0/\partial x = -w_0$ from $-\infty$ to x with respect to x gives the zeroth-order perturbation streamfunction φ_0:

$$\varphi_0(x, z) = \begin{cases} -X_3(1 - \sin d \sin z - \cos z) \\ \quad - (1 - \cos d)X_4 \sin z & \text{for} \quad 0 \leqslant z \leqslant d \quad (29a) \\ (1 - \cos d)(X_3 \cos z - X_4 \sin z) & \text{for} \quad z > d, \quad (29b) \end{cases}$$

where

$$X_3 = a_1\left(\tan^{-1}\frac{x}{a_1} - \tan^{-1}\frac{x}{a_2}\right)$$

$$X_4 = \frac{a_1}{2} \ln\left(\frac{x^2 + a_1^2}{x^2 + a_2^2}\right).$$

The zeroth-order perturbation horizontal wind u_0 is obtained by differentiating φ_0 with respect to z:

$$u_0(x, z) = \begin{cases} X_3(\sin d \cos z - \sin z) \\ \quad - (1 - \cos d)X_4 \cos z & \text{for} \quad 0 \leqslant z \leqslant d \quad (30a) \\ -(1 - \cos d)(X_3 \sin z + X_4 \cos z) & \text{for} \quad z > d. \quad (30b) \end{cases}$$

From (18), it follows that the zeroth-order perturbation buoyancy b_0 is given by

$$b_0(x, z) = \varphi_0(x, z) + \int_{-\infty}^{x} q_0(x, z)dx, \quad (31)$$

which yields

$$b_0(x, z) = \begin{cases} -X_3(1 - \sin d \sin z - \cos z) \\ \quad - (1 - \cos d)X_4 \sin z + X_3 & \text{for} \quad 0 \leqslant z \leqslant d \quad (32a) \\ (1 - \cos d)(X_3 \cos z - X_4 \sin z) & \text{for} \quad z > d. \quad (32b) \end{cases}$$

c. First-order solutions

To solve the first-order equation (22), we need to evaluate the forcing term $F(x, z)$ resulting from the zeroth-order solutions. For $0 \leqslant z \leqslant d$,

$$\begin{aligned} F(x, z) &= -J(\varphi_0, -2b_0) && \text{from (23) and (17)} \\ &= 2J(\varphi_0, b_0) && \text{using Jacobian identity} \\ &= 2J(\varphi_0, \varphi_0 + X_3) && \text{from (31) and } X_3 \\ &= 2J(\varphi_0, X_3) && \text{using Jacobian identity} \\ &= -2u_0\partial X_3/\partial x && \text{since } \partial X_3/\partial z = 0 \text{ and} \\ & && \partial\varphi_0/\partial z = u_0. \end{aligned}$$

Therefore,

$$F(x, z) = -2X_1[X_3(\sin d \cos z - \sin z) - (1 - \cos d)X_4 \cos z]. \quad (33)$$

For $z > d$, $F(x, z) = 0$.

Taking the Fourier transform of (22) yields

$$\frac{\partial^2 \tilde{w}_1}{\partial z^2} + \tilde{w}_1 = \tilde{F}. \quad (34)$$

The general solution to (34) is

$$\tilde{w}_1(k,z)=\begin{cases}A_1(k)e^{iz}+B_1(k)e^{-iz}+\tilde{w}_{1p}(k,z) & \text{for}\quad 0\le z\le d \quad (35a)\\ C_1(k)e^{iz}+D_1(k)e^{-iz} & \text{for}\quad z>d, \quad (35b)\end{cases}$$

where $\tilde{w}_{1p}$ represents a particular solution. Since the homogeneous solution is known, the particular solution may be written as (Hildebrand 1976)

$$\tilde{w}_{1p}(k,z)=\alpha_1(k,z)e^{iz}+\alpha_2(k,z)e^{-iz}, \quad (36)$$

where

$$\alpha_1(k,z)=-\int\frac{\tilde{F}(k,z)e^{-iz}}{W(e^{iz},e^{-iz})}dz$$

$$\alpha_2(k,z)=\int\frac{\tilde{F}(k,z)e^{iz}}{W(e^{iz},e^{-iz})}dz.$$

Here, the symbol W denotes the Wronskian defined by $W(C,D)=C(dD/dz)-D(dC/dz)$. Since $W(e^{iz}, e^{-iz})=-2i$ and an interchange of integrals gives the same result, the particular solution can be expressed by

$$\tilde{w}_{1p}(k,z)=-\frac{ie^{iz}}{2\pi}\int_{-\infty}^{\infty}S(x,z)e^{-ikx}dx+\frac{ie^{-iz}}{2\pi}\int_{-\infty}^{\infty}T(x,z)e^{-ikx}dx, \quad (37)$$

where

$$S(x,z)=\int F(x,z)e^{-iz}dz$$

$$T(x,z)=\int F(x,z)e^{iz}dz.$$

The $\tilde{w}_{1p}$ in (37) is equivalent to [see (24a)]

$$\tilde{w}_{1p}(k,z)=-\frac{ie^{iz}}{2}\tilde{S}(k,z)+\frac{ie^{-iz}}{2}\tilde{T}(k,z). \quad (38)$$

Using (33), the functions $S(x,z)$ and $T(x,z)$ for $0\le z\le d$ can be shown to be

$$\begin{aligned}S(x,z)=-\frac{X_1}{2}\{&X_3[(2z+\sin 2z)\sin d+\cos 2z]\\&-(1-\cos d)X_4(2z+\sin 2z)\\&+i[X_3(\sin d\cos 2z+2z-\sin 2z)\\&\quad-(1-\cos d)X_4\cos 2z]\}, \quad (39)\end{aligned}$$

$$\begin{aligned}T(x,z)=-\frac{X_1}{2}\{&X_3[(2z+\sin 2z)\sin d+\cos 2z]\\&-(1-\cos d)X_4(2z+\sin 2z)\\&-i[X_3(\sin d\cos 2z+2z-\sin 2z)\\&\quad-(1-\cos d)X_4\cos 2z]\}. \quad (40)\end{aligned}$$

Notice that $S(x,z)$ and $T(x,z)$ are zero for $z>d$.

As was done previously for the zeroth-order solution w_0, the lower-boundary condition of $\tilde{w}_1=0$ at $z=0$, the upper radiation condition $[D_1(k)=0]$, and the interface conditions of continuity of $\tilde{w}_1$ and $\partial\tilde{w}_1/\partial z$ at $z=d$ are imposed to determine the four coefficients $A_1(k)$, $B_1(k)$, $C_1(k)$, and $D_1(k)$. After some manipulation, the solution for the first-order vertical velocity $\tilde{w}_1$ field is given by

$$\begin{aligned}\tilde{w}_1(k,z)=\frac{i}{2}\Bigg\{&\Bigg[2i(\tilde{S}(k,0)-\tilde{T}(k,0)+\tilde{T}(k,d))\\&+e^{2id}\frac{\partial\tilde{S}(k,d)}{\partial z}-\frac{\partial\tilde{T}(k,d)}{\partial z}\Bigg]\sin z\\&+(\tilde{S}(k,0)-\tilde{T}(k,0))e^{-iz}-e^{iz}\tilde{S}(k,z)\\&+e^{-iz}\tilde{T}(k,z)\Bigg\}\quad \text{for}\ 0\le z\le d, \quad (41a)\end{aligned}$$

$$\begin{aligned}\tilde{w}_1(k,z)=\frac{i}{2}\Bigg\{&\tilde{S}(k,0)-\tilde{T}(k,0)-\tilde{S}(k,d)\\&+\tilde{T}(k,d)-\frac{i}{2}(1-e^{-2id})\\&\times\left[e^{2id}\frac{\partial\tilde{S}(k,d)}{\partial z}-\frac{\partial\tilde{T}(k,d)}{\partial z}\right]\Bigg\}e^{iz}\\&\text{for}\quad z>d. \quad (41b)\end{aligned}$$

Notice that the analytical forms of $\partial S(x,z)/\partial z$ and $\partial T(x,z)/\partial z$ can be obtained from (39) and (40), and $\partial\tilde{S}(k,d)/\partial z$ and $\partial\tilde{T}(k,d)/\partial z$ mean that $\partial\tilde{S}(k,z)/\partial z$ and $\partial\tilde{T}(k,z)/\partial z$ are evaluated at $z=d$. The solutions for $\tilde{\varphi}_1$, $\tilde{u}_1$, and $\tilde{b}_1$ can be obtained by taking the Fourier transforms of $\partial\varphi_1/\partial x=-w_1$, $\partial u_1/\partial x+\partial w_1/\partial z=0$, and (20), which yield

$$\tilde{\varphi}_1(k,z)=\frac{i}{k}\tilde{w}_1(k,z), \quad (42)$$

$$\tilde{u}_1(k,z)=\frac{i}{k}\frac{\partial\tilde{w}_1(k,z)}{\partial z}, \quad (43)$$

$$\tilde{b}_1(k,z)=\tilde{\varphi}_1(k,z)-\frac{i}{k}\tilde{J}(\varphi_0,b_0). \quad (44)$$

Equation (44) is equivalent to

$$\tilde{b}_1(k,z)=\tilde{\varphi}_1(k,z)-\frac{i}{2k}\tilde{F}(k,z). \quad (45)$$

The term $\partial\tilde{w}_1/\partial z$ is obtained analytically from (41a) and (41b). Then, taking the inverse Fourier transforms of $\tilde{w}_1$, $\tilde{\varphi}_1$, $\tilde{u}_1$, and $\tilde{b}_1$ yields the required solutions for w_1, φ_1, u_1, and b_1 [see (24b)].

Since the functions $S(x,z)$ and $T(x,z)$ [(39) and (40)] contain the $2z$ term, the solution w_1 also contains the $2z$ term. Therefore, the magnitude of w_1 can be larger than O(1) for large values of the nondimensional heating depth d or the inverse Froude number. This might violate the very first assumption of the perturbation expansion. However, because $S(x, z)$ and $T(x, z)$ are bounded mathematically by $z = d$ and in the real atmosphere the heating depth due to, for example, cumulus convection is confined to a region below the tropopause, the solution w_1 is not overly constrained by the $2z$ term. This constraint can be further relaxed when the atmosphere is less stable (smaller N) and when the basic-state horizontal wind speed increases (larger U). However, we should still choose a proper range of d over which the solution does not violate the assumption of the perturbation expansion.

A fast Fourier transform (FFT) algorithm is employed to get the first-order solutions numerically. For this, the known functions $F(x, z)$, $S(x, z)$, $T(x, z)$, $\partial S(x, z)/\partial z$, and $\partial T(x, z)/\partial z$ [see (33), (39), and (40)] are forward-transformed ($x \rightarrow k$). Then, $\tilde{w}_1$, $\tilde{\varphi}_1$, $\tilde{u}_1$, and $\tilde{b}_1$ are evaluated in Fourier space using (41a)–(43) and (45). Finally, $\tilde{w}_1$, $\tilde{\varphi}_1$, $\tilde{u}_1$, and $\tilde{b}_1$ are backward-transformed ($k \rightarrow x$) to give w_1, φ_1, u_1, and b_1 in physical space. The accuracy of the numerical solutions obtained by the FFT will be demonstrated by comparison with the zeroth-order analytical solution in section 4. For all the calculations, the total number of horizontal waves specified over a horizontal domain size of 51.1 are 512 and a vertical domain size is 10 with a vertical resolution of 0.1. The large horizontal domain is chosen so that the impact of the periodic boundary condition implied by the FFT can be reduced. A very large number of horizontal waves are chosen so that accurate solutions can be obtained. The nondimensional length scales a_1 and a_2 are set to 1 and 5, respectively.

3. Energy argument

Using the governing equations for the zeroth-order perturbations, one can derive the zeroth-order wave energy equation

$$\frac{\partial}{\partial x}(E_0 + \pi_0 u_0) + \frac{\partial}{\partial z}(\pi_0 w_0) = b_0 q_0, \qquad (46)$$

where E_0 $[=(u_0^2 + b_0^2)/2]$ is the zeroth-order total wave energy. The above equation indicates that in the absence of vertical wind shear the source of the zeroth-order wave energy comes from the diabatic forcing. Equation (46) is identical to the nondimensional form of (33) in Lin (1987) in the absence of vertical wind shear. Therefore, arguments for the negative phase relationship between the momentum flux and vertical energy flux and vertical variation of momentum flux are the same as those given in Lin (1987). The only reason we present (46) is to investigate the connection between the zeroth-order and the first-order wave energy.

Using the governing equations for the first-order perturbations, the first-order wave energy equation can be derived and is given by

$$\frac{\partial}{\partial x}(E_1 + \pi_1 u_1) + \frac{\partial}{\partial z}(\pi_1 w_1) = -u_1\left(\frac{\partial E_0}{\partial x} - b_0 q_0\right) + \frac{b_1 F}{2}. \qquad (47)$$

Here, E_1 is the first-order total wave energy defined by $E_1 = (u_1^2 + b_1^2)/2$. There are three source terms for the first-order wave energy. The terms on the right-hand side of (47) result from nonlinear interactions between the zeroth-order and the first-order perturbations. The first term represents the horizontal advection of the zeroth-order total wave energy by the first-order perturbation horizontal wind. The second term is somewhat difficult to interpret physically. From (46), it can be seen that the two terms inside parentheses on the right-hand side of (47) represent the convergence of wave energy flux. The third term represents the connection with the forcing to the first-order equation, which is similar to the $b_0 q_0$ term in (46).

Above the forcing region ($z > d$), the only source for the first-order wave energy is the horizontal advection of the zeroth-order total wave energy (E_0). The E_0 can be calculated analytically using (30) and (32). Above the forcing region, E_0 is shown to be given by

$$E_0 = \frac{1}{2}(1 - \cos d)^2 (X_3^2 + X_4^2). \qquad (48)$$

The zeroth-order total wave energy above the forcing region is independent of height as shown in Eliassen and Palm (1960). In the forcing region ($0 \leq z \leq d$), the forcing of q_0 and F exist together with the zeroth-order total wave energy advection. The E_0 in the forcing region is dependent upon height as given by (30a) and (32a). The source term $b_0 q_0$ is negative on the upstream edge of the heating and positive on the downstream because the sign of b_0 is determined by the horizontal integration of q_0 from far upstream. This is also true in the $b_1 F$ term because F produces positive b_1 on the upstream and negative b_1 on the downstream. The magnitude and vertical structure of each first-order wave energy source term are shown in Figs. 10 and 11.

4. Results and discussion

All the first-order solutions in physical space presented in this section are obtained from the FFT of the analytic solutions in wavenumber space. Accordingly, the accuracy of the numerical solutions obtained by the FFT should be checked first. Figure 1 shows two zeroth-order (linear) perturbation vertical velocity fields, one obtained from the fully analytical solution and the other from the inverse Fourier transform of the solution in wavenumber space using the FFT routine. In the both cases, the nondimensional heating depth d is specified as 1. All the solutions are in nondimensional form. Hereafter, all the figures are presented in nondimensional domain with nondimensional values. The mag-

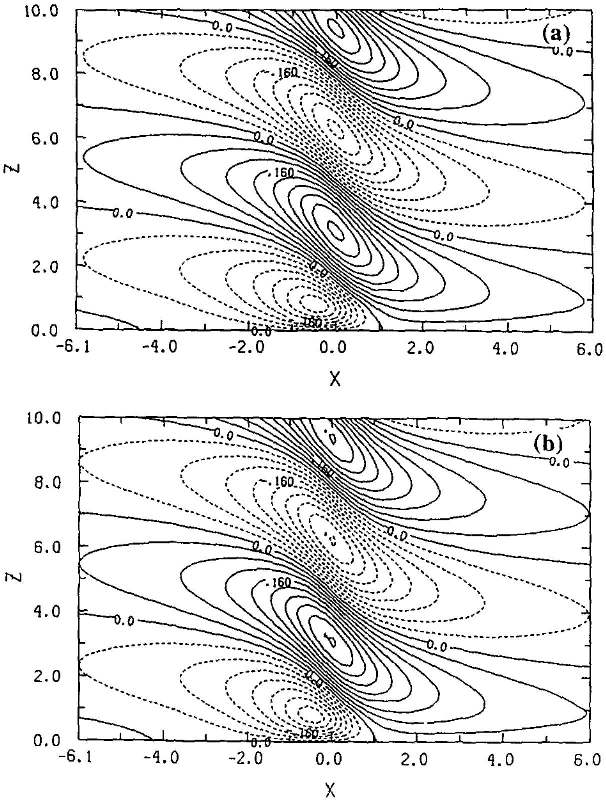

FIG. 1. The zeroth-order perturbation vertical velocity fields obtained from (a) the analytical solution of (28a) and (28b) and (b) the inverse Fourier transform of the solution in wavenumber space given by (27a) and (27b) using the FFT algorithm for the case of $d = 1$. Contour interval is 0.04.

nitude and phase in these two fields are so well matched to each other that the solution by the FFT might be considered as the analytical solution, hence crediting the numerical solutions for the first-order perturbations presented below.

Figure 2 shows fields of the specified heating q and the forcing function F [see (23) and (33)] to the first-order equation for the case of $d = 1$. Unlike the specified heating field, the forcing function represents cooling concentrated in the specified heating region. The cooling is tilted slightly upstream because it is calculated using the zeroth-order solutions, which are also tilted slightly upstream. From (33), the integration of the term involving X_1X_3 on the right-hand side from $x = -\infty$ to ∞ is zero because X_1X_3 is an odd function. However, the horizontal integration of the term involving X_1X_4 is not zero. Since an analytical evaluation of this integral seems to be quite complicated, a numerical integration of X_1X_4 is performed using a cubic spline routine over the entire horizontal domain, that is, from $x = -25.55$ to 25.55. The calculated value is -1.85. Of course, this value might be changed slightly when a wider horizontal domain is used. In order to check the accuracy of the cubic spline routine and the influence of the horizontal domain size, an integration of X_1X_3 over the same horizontal domain was done using the same numerical program. The integrated value was 8.95×10^{-8}, which is in acceptable agreement with the analytical value of 0.

Hence, the sign of the horizontal integration of F is determined by the $\cos z$ term because $(1 - \cos d)$ is always positive or zero. Therefore, the integral can be positive, zero, or negative depending on the magnitude of d in the forcing region. This implies that the net forcing to the first-order equation is zero when $d = 2\pi$, 4π, 6π, $\cdots$. In addition, the net forcing is zero at the specific heights of $z = \pi/2$, $3\pi/2$, $5\pi/2$, $\cdots$ below $z = d$. Therefore, except for these specific heating depths and heights, the forcing F can have a net horizontal heating or cooling in general. Even though the forcing itself is localized near the center of the prescribed heating, the first-order vertical displacement, pressure, and temperature fields may not be bounded at infinity (Smith and Lin 1982) except for the specific heights at which the net forcing becomes zero.

Figure 3 shows the first-order (weakly nonlinear) perturbation vertical velocity field for the case of

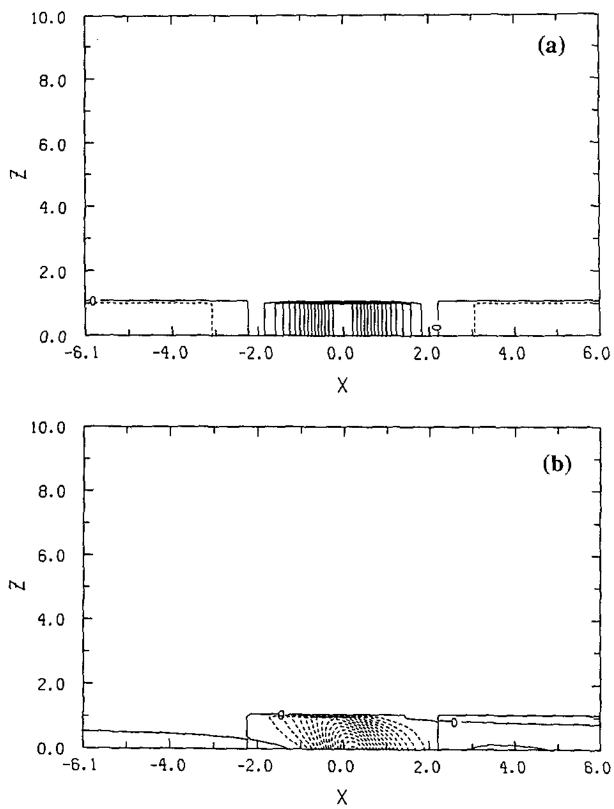

FIG. 2. The fields of (a) the specified heating q [(13) and (14)] and (b) the forcing function F to the first-order equation [(33)] for the case of $d = 1$. Contour intervals in (a) and (b) are 0.05 and 0.08, respectively.

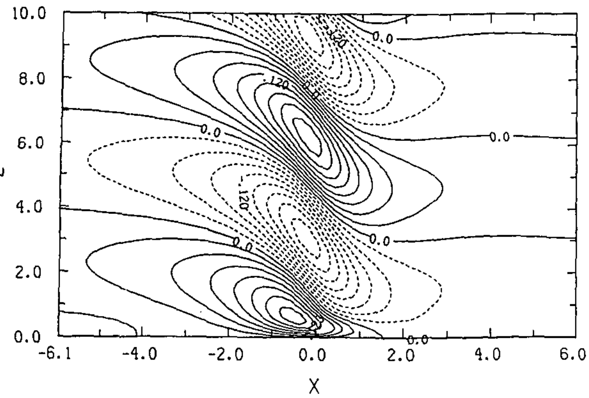

FIG. 3. The first-order perturbation vertical velocity field for the case of $d = 1$. Contour interval is 0.03.

$d = 1$. In the corresponding zeroth-order field (Fig. 1), there is downward motion along the upstream side of the specified heating region and upward motion along the downstream. Notice that the nondimensional vertical wavelength [$\lambda_z = \lambda_z^*/(U/N) = (2\pi U/N)/(U/N) = 2\pi$, where λ_z^* is the dimensional vertical wavelength] is independent of the nondimensional heating depth. In the first-order field, there is upward motion in the center that extends to the upstream side of the forcing (cooling in this case) region. The zeroth-order solution field is symmetric with respect to the upstream tilt, while the first-order solution field is asymmetric. This is because the forcing F to the first-order equation is not horizontally symmetric, as shown in Fig. 2b. The strong upward motion in the center of the domain near the surface is associated with strong convergence there through the continuity equation.

The first-order solution represents the linear response of a stably stratified atmosphere to localized cooling. However, this response is different from that produced by the specified cooling prescribed by Lin and Chun (1991). The difference comes mainly from the fact that the horizontal and vertical structure of the forcing was *specified* in their case and ours is *determined by the zeroth-order perturbations.* In their case, the flow response to the cooling is just opposite to the zeroth-order solution in the present case for the same Froude number because the horizontal and vertical structure of the cooling they used is the same as the heating we specified in the zeroth-order equations.

Figure 4 shows the zeroth- and first-order perturbation buoyancy fields for the case of $d = 1$. Since the diabatic forcing q_0 in the b_0 field and the forcing F in the b_1 field are discontinuous at $z = d$, the buoyancy fields are discontinuous at that level. The buoyancy perturbations arise in two ways, one directly from the horizontal integration of the diabatic forcing from far upstream and the other indirectly from the thermally generated streamfunction or vertical velocity field. In the b_0 field, the value of the horizontally integrated diabatic forcing X_3 is negative for $x < 0$, zero at $x = 0$, positive for $x > 0$, and maximum at $x = (a_1a_2)^{1/2}$. Therefore, the combination of X_3, which is vertically uniform in the forcing region, and the upstream-tilted streamfunction field produces the upstream-tilted buoyancy field in the forcing region. The sign of the vertical velocity seems to be determined by the sign of the buoyancy field. Maximum upward motion takes place when the parcel receives the maximum amount of heat just before cooling begins as mentioned in Smith and Lin (1982). In the b_1 field, the integrated forcing has two parts, one from the integration of X_1X_3 and the other from X_1X_4. Even though this evaluation is somewhat complicated compared with the zeroth-order case, the resultant effect is almost identical to negative X_3 since F represents a localized cooling in the specified heating region.

In the present weakly nonlinear flow system, the nonlinearity cannot be too large. On the upstream side of the forcing region, the first-order upward motion cannot overcome the zeroth-order downward motion. Although the total field (e.g., $w_0 + \mu w_1$) for arbitrary selected μ is not shown, it is very similar to the zeroth-order solution for small values of μ. However, as the nonlinearity increases, the magnitude of the first-order

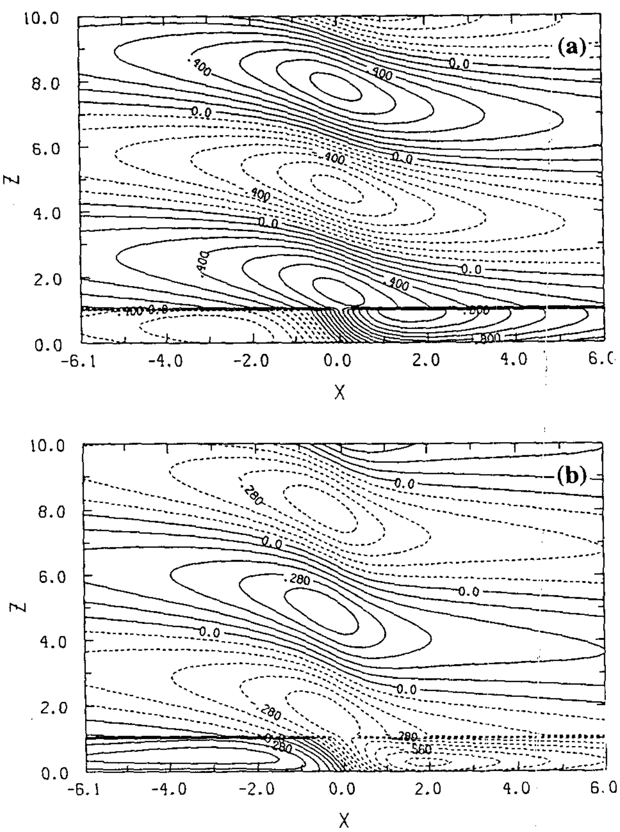

FIG. 4. The perturbation buoyancy fields of (a) the zeroth order and (b) the first order for the case of $d = 1$. Contour intervals in (a) and (b) are 0.1 and 0.07, respectively.

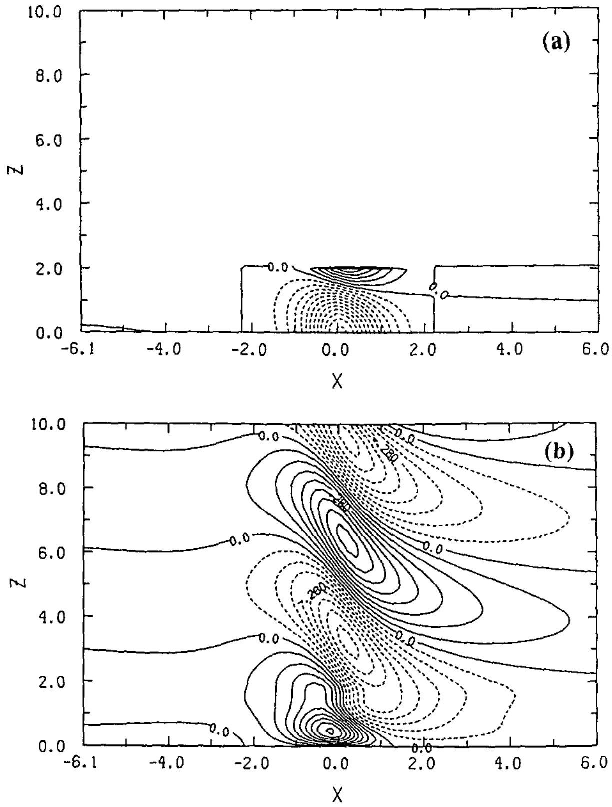

FIG. 5. The fields of (a) the forcing function F and (b) the first-order perturbation vertical velocity for the case of $d = 2$. Contour intervals in (a) and (b) are 0.3 and 0.07, respectively.

motion can increase faster than the zeroth-order motion. Therefore, the first-order upward motion may overcome the zeroth-order downward motion near the center of the prescribed heating. Using a linear numerical model, Raymond (1986) also showed that the cooling suppresses the subsidence produced by heating and allows parcels from near the surface to rise to the level of free convection. This process is required for the wave–CISK. The cooling he used is prescribed, while in this study it is determined by the zeroth-order perturbations. In the weakly nonlinear case, the cooling generated by the linear waves induced by the heating plays a similar role to the additional cooling in the linear study by Raymond. In the real atmosphere, the combined effects of rain-produced cooling and linear wave-induced cooling may act together to enhance the upstream upward motion in the lower layer, which is important for the generation of convection.

Figure 5a shows the forcing function F for the case of $d = 2$. As mentioned before, there is a cooling region with an upstream tilt below $z \sim \pi/2$ and a heating region above because F changes its sign depending on the $\cos z$ term in the forcing region. Figure 5b shows the first-order perturbation vertical velocity field for this case. The upward motion is stronger than that in the $d = 1$ case. Even though the nondimensional heating depth d is not explicitly involved in the nonlinearity factor μ [see (12)], the magnitude of d is implicitly related to μ because d is nondimensionalized by U/N. If N is fixed, an increase in d means a decrease in U for a fixed dimensional heating depth, which results in an increase of μ by a factor of $1/U^2$. If both U and N are fixed, an increase in d implies an increase in the dimensional heating depth. In this case, we consider taller cloud, which has a larger amount of total latent heating because of the constant heating rate q_0. Since both U and N are included in the scaling factor, an increase in d may be more properly interpreted as an increase in the dimensional heating depth.

Figure 6 shows the zeroth- and first-order perturbation horizontal velocity fields for the case of $d = 2$. In the u_0 field, there is low-level horizontal divergence upstream and low-level horizontal convergence downstream. These regions of divergence and convergence are associated with the downward and upward motion, respectively, as shown in Fig. 5b. On the other hand, strong convergence exists in the u_1 field at $x = 0$ near the surface and much weaker divergence aloft; this strong convergence produces the upward motion that is located there.

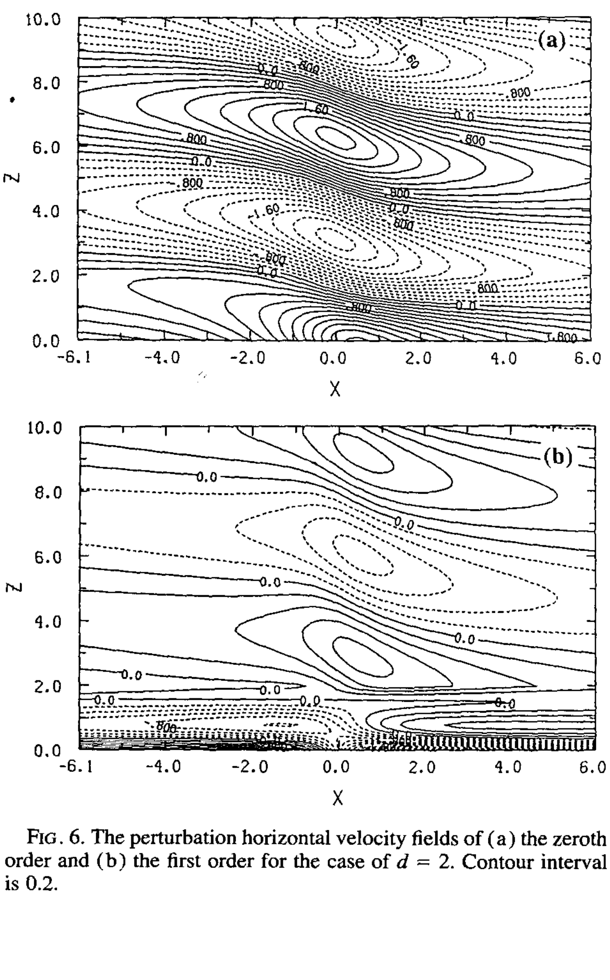

FIG. 6. The perturbation horizontal velocity fields of (a) the zeroth order and (b) the first order for the case of $d = 2$. Contour interval is 0.2.

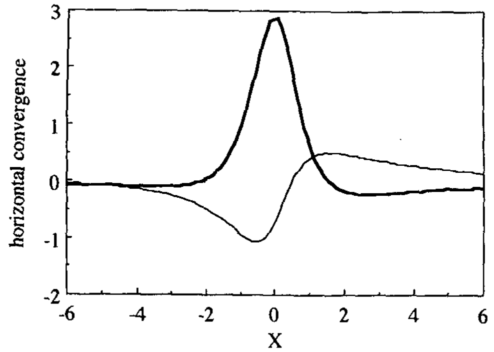

FIG. 7. The horizontal convergence of the zeroth order (thin line) and the first order (thick line) at the surface for the case of $d = 2$.

Figure 7 shows the zeroth-order ($-\partial u_0/\partial x$) and the first-order ($-\partial u_1/\partial x$) horizontal convergence at the surface for the case of $d = 2$. From (30a), the term $-\partial u_0/\partial x$ can be analytically expressed by $-X_1 \sin d + (1 - \cos d)X_2$. This gives divergence upstream and convergence downstream, which is consistent with Fig. 6a. On the other hand, the term $-\partial u_1/\partial x$ represents a region of strong convergence in the center of the forcing. The maximum value of the convergence is about three times larger than that of the divergence for the zeroth-order perturbation. This strong convergence in the forcing center is responsible for upward motion there. It is interesting to notice that the horizontal convergence at $z = 0$ induced by the first-order perturbation is almost opposite to that for stratified hydrostatic flow over an isolated bell-shaped mountain, even though the vertical velocity field is similar to that characterizing mountain waves.

In fact, for all values of d, the first-order perturbation is forced by the cooling near the surface induced by the zeroth-order perturbations that produce strong convergence in the center of the forcing region. Even though the first-order solution represents the linear flow response to the isolated cooling, it is different from that in Lin and Chun (1991) because the cooling generated by the Jacobian of the zeroth-order solutions has a different form. One of the main nonlinear effects on gravity waves induced by prescribed heating is that the linear solution generated by the heating produces the cooling for the first-order equation, which produces the strong convergence near the surface. This convergence is responsible for generating upward motion in the center and upstream of the forcing region and compensates for the zeroth-order perturbation downward motion there. The relative magnitude of the upward and downward motion can be determined by the nondimensional heating depth or the inverse Froude number.

It is remarkable that the sign of F in (33) is the same even if a specified cooling in the zeroth-order equation is used instead of specified heating. This is because both signs of u_0 and $\partial X_3/\partial x$ are changed when the heating is replaced by cooling. This means that the weakly nonlinear perturbations always produce convergence near the surface regardless of the specified forcing type. This implies that the weakly nonlinear effect is equivalent to prescribing an additional forcing in the linear system.

Even though the weakly nonlinear theory presented here is not applicable to fully nonlinear situations, it does provide valuable insights into the nonlinear response of a stably stratified flow to prescribed thermal forcing. Notice, however, that the theory is formulated under several assumptions. Perhaps the most serious restriction to the applicability of our solutions lies in the value of the nondimensional heating depth or the inverse Froude number. Since $S(x, z)$ and $T(x, z)$ in the first-order solutions include the $2z$ term for $0 \leqslant z \leqslant d$, d should be small enough to constrain the magnitude of the first-order solution to be within order one.

Figure 8 shows the domain maximum zeroth- and first-order vertical velocities as a function of d. The maximum vertical velocity in the first-order solution exhibits oscillatory behavior with larger amplitudes for larger values of d. Also, there is a period of 2π in the w_1 maximum graph because the net forcing F is maximum at $d = \pi, 3\pi, 5\pi, \cdots$ and zero at $d = 2\pi, 4\pi, 6\pi, \cdots$. The domain maximum zeroth- and first-order perturbation horizontal velocities as a function of d is shown in Fig. 9. The maximum horizontal velocity has the same trend as the maximum vertical velocity. In the u_0 maximum graph, there is also a period of 2π that is not clearly seen in the w_0 maximum graph (Fig. 8). This 2π period is related to the $(1 - \cos d)$ term in (28) and (30). From these figures, the weakly nonlinear solutions appear to be valid up to $d = 3$.

Figure 10 shows the vertical profiles of the source term ($-u_1 \partial E_0/\partial x$) in the first-order wave energy equation outside the forcing region at $x = -1$, 0, and 1 for the case of $d = 1$. The magnitude of this term is slightly

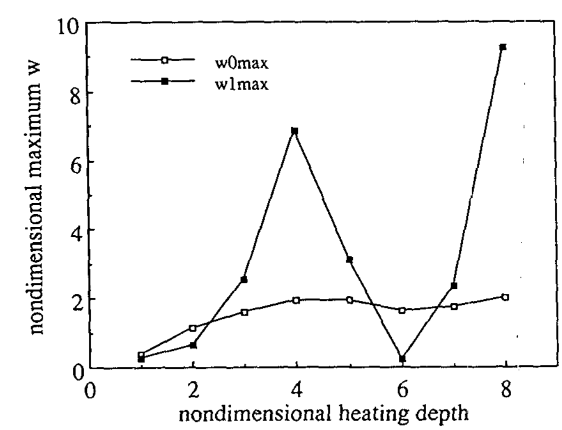

FIG. 8. The domain maximum perturbation vertical velocities of the zeroth order (w0 max) and the first order (w1 max) as a function of d.

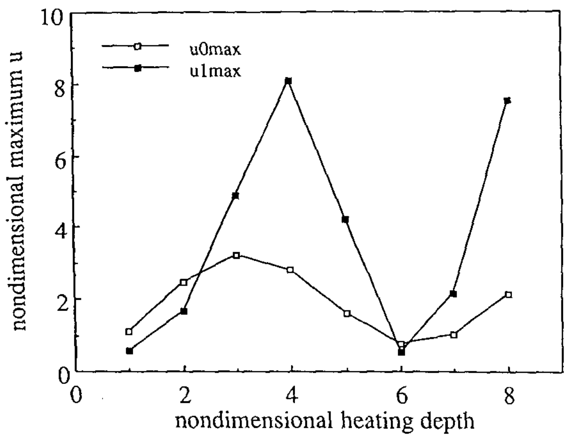

FIG. 9. The domain maximum perturbation horizontal velocities of the zeroth order (u0 max) and the first order (u1 max) as a function of d.

larger on the upstream side than that on the downstream side because u_1 is shifted upstream with respect to the upstream phase tilt. This is opposite in the case of $d = 2$ by the downstream-shifted u_1 field as shown in Fig. 6b. This is because the forcing F is not horizontally symmetric.

Figure 11 shows the vertical profiles of the three individual source terms and their total in the first-order wave energy equation inside the forcing region at $x = -1$, 0, and 1 for the case of $d = 1$. The first term is relatively small and negative above $z \sim 0.3$ on the upstream side, positive at the center, and positive on the downstream side. The second and third terms tend to cancel each other except for the region near the surface. Therefore, the total contribution from these three source terms is approximately the same as the first term, at least in sign. The magnitude of the total wave energy source increases on the downstream side near the surface.

5. Summary and conclusions

The weakly nonlinear response of a two-dimensional stably stratified atmosphere to prescribed heating in a uniform flow was considered analytically. The prescribed heating was assumed to have only a zeroth-order term that was specified to be vertically homogeneous from the surface to a certain height and bell shaped in the horizontal. A perturbation expansion in a small value of the nonlinearity factor for the thermally induced waves was performed. The resulting two highest-order linear governing equations [zeroth-order (linear) and first-order (weakly nonlinear)] were solved. The zeroth-order solutions were obtained analytically in physical space, while the first-order solutions were obtained analytically in wavenumber space and transformed back to physical space numerically using the FFT algorithm.

It was shown that the nondimensional heating depth (d) or the inverse Froude number should be relatively small (<3) in order to have valid first-order solutions in terms of the perturbation expansion. The zeroth-order solutions are dependent upon the inverse Froude number as shown in previous studies (Smith and Lin 1982; Lin and Smith 1986; Lin 1987).

The forcing (F) to the first-order equation induced by the Jacobian of the zeroth-order solutions has a vertical structure in the specified heating region because of a 2π vertical wavelength of the zeroth-order solution with an upstream tilt. However, F always produces cooling in the lower layer regardless of the nondimensional heating depth and whether the specified forcing in the zeroth-order equation is heating or cooling. The induced cooling in the lower layer produces strong convergence near the surface in the center of the forcing. This convergence is responsible for generating upward motion in the center and on the upstream side of the forcing region through the mass continuity, which reduces the zeroth-order downward motion. The response of the atmosphere to this type of cooling is different from that found by Lin and Chun (1991) mainly be-

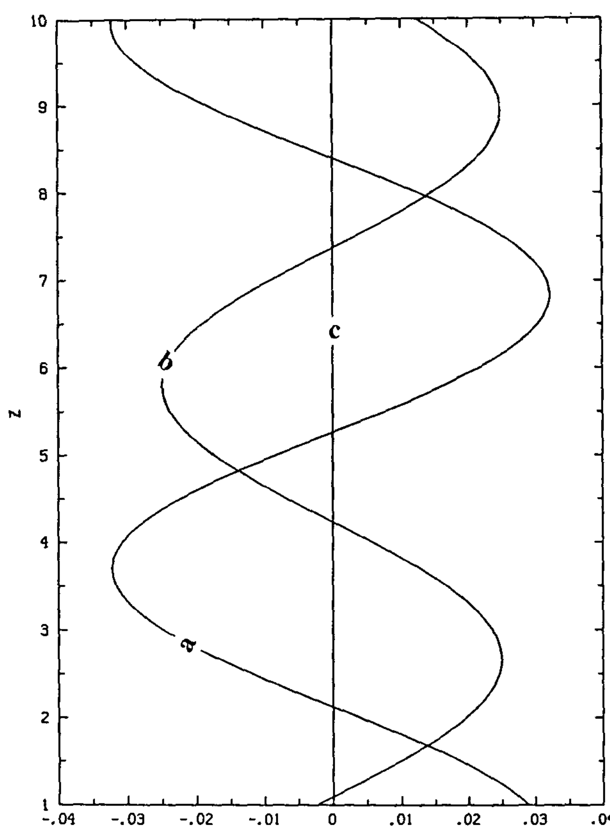

FIG. 10. The vertical profiles of the source term ($-u_1 \partial E_0/\partial x$) in the first-order wave energy equation outside the specified forcing region ($z > d$) for the case of $d = 1$. Curves a, b, and c indicate profiles at $x = -1$, 1, and 0, respectively.

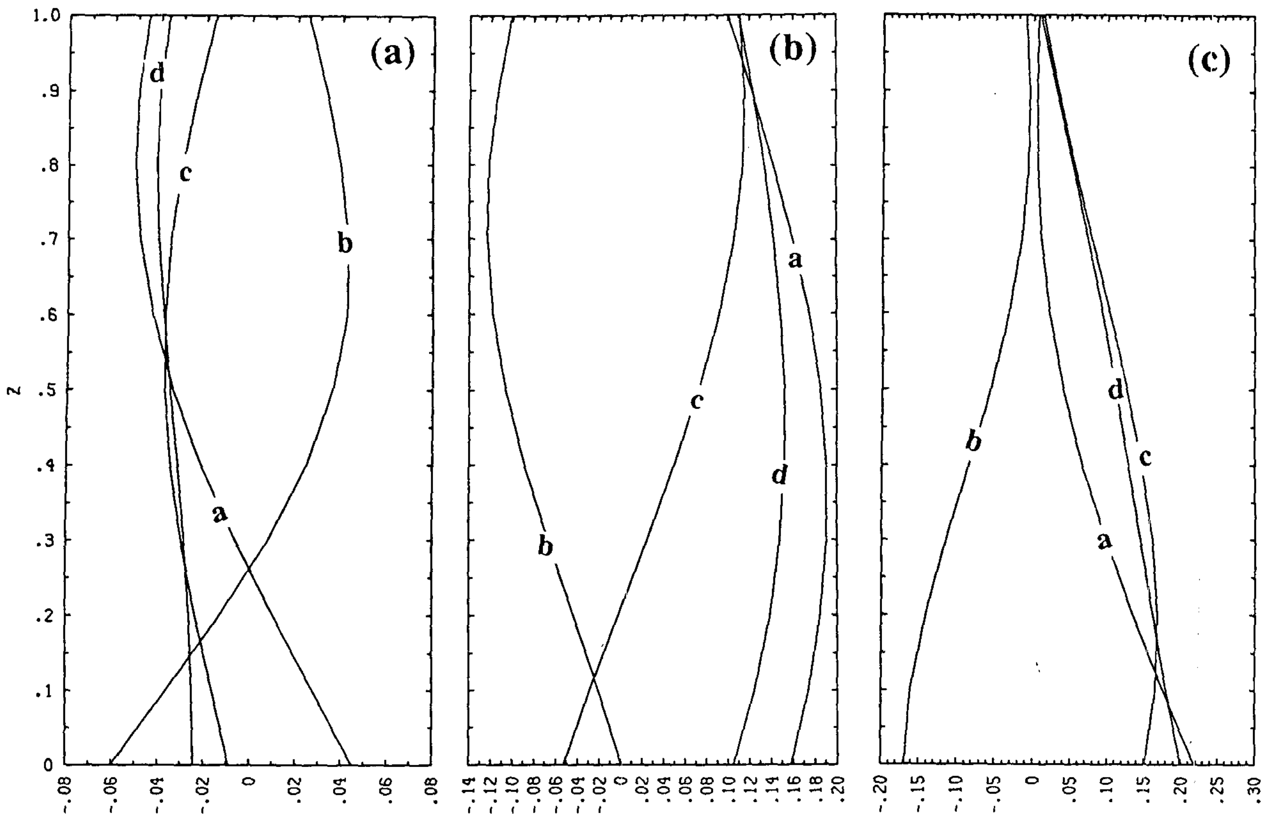

FIG. 11. The vertical profiles of the three source terms and their total in the first-order wave energy equation inside the forcing region ($0 \leq z \leq d$) at (a) $x = -1$, (b) $x = 0$, and (c) $x = 1$ for the case of $d = 1$. Curves a, b, c, and d in each figure indicate the first, second, third, and total of these three source terms in (47), respectively.

cause the horizontal and vertical structure of the forcing is different. In their case, the linear response of a two-dimensional stratified atmosphere to specified cooling is just opposite to that produced by heating for the same Froude number because the horizontal and vertical structure of the cooling is the same as that of the heating used in our case. In some sense, the weakly nonlinear response of a two-dimensional stably stratified atmosphere to prescribed heating is equivalent to the linear response to combined heating and additional weak cooling.

The wave energy equations for the zeroth-order and the first-order perturbations were presented. Above the forcing region, the wave energy source for the first-order perturbation is the horizontal advection of the zeroth-order total wave energy by the first-order perturbation horizontal velocity. In the specified forcing region, there are three source terms, which represent nonlinear interactions between the zeroth-order and the first-order waves. However, the total of these three terms is nearly the same as the term representing the horizontal advection of the zeroth-order total wave energy by the first-order perturbation horizontal wind due to cancellation between the other two terms.

In this study, we considered the steady-state, weakly nonlinear response of a two-dimensional stably stratified atmospheric flow to specified heating in a uniform flow. In the real atmosphere, the flow is strongly time dependent and highly nonlinear in most cases. Therefore, there is a limitation in the application of this study to response of real atmospheric flows. In addition, the applicability of the weakly nonlinear approach is only valid when the flow system is characterized by relatively large values of the Froude number. However, this study provides a basic picture of the weakly nonlinear response to diabatic forcing. The main nonlinear effect on the flow is that cooling induced by diabatic heating (or cooling) produces convergence near the surface, thus providing a mechanism for the generation of upward motion in the center of the forcing region that extends upstream. Wind shear effects will be investigated in the future.

Acknowledgments. The authors would like to thank Yuh-Lang Lin and Ron Weglarz for providing valuable comments on this study. This research was partly supported by the Korea Ministry of Environment under the project of Research and Development on Technology for Global Environmental Monitoring and Climate

Change Prediction, and the Korea Ministry of Science and Technology (93).

REFERENCES

Baik, J.-J., 1992: Response of a stably stratified atmosphere to low-level heating—An application to the heat island problem. *J. Appl. Meteor.*, **31**, 291–303.

Barcilon, A., and D. Fitzjarrald, 1985: A nonlinear steady model for moist hydrostatic mountain waves. *J. Atmos. Sci.*, **42**, 58–67.

Booker, J. R., and F. R. Bretherton, 1967: The critical layer for internal gravity waves in a shear flow. *J. Fluid Mech.*, **27**, 513–539.

Bretherton, C., 1988: Group velocity and the linear response of stratified fluids to internal heat or mass sources. *J. Atmos. Sci.*, **45**, 81–93.

Eliassen, A., and E. Palm, 1960: On the transfer of energy in stationary mountain waves. *Geophys. Publ.*, **22**, 1–23.

Hildebrand, F. B., 1976: *Advanced Calculus for Applications*. Prentice-Hall, 733 pp.

Lin, C. A., and R. E. Stewart, 1991: Diabatically forced mesoscale circulations in the atmosphere. *Advances in Geophysics*, Vol. 33, Academic Press, 267–305.

Lin, Y.-L., 1987: Two-dimensional response of a stably stratified shear flow to diabatic heating. *J. Atmos. Sci.*, **44**, 1375–1393.

——, 1990: A theory of cyclogenesis forced by diabatic heating. Part II: A semigeostrophic approach. *J. Atmos. Sci.*, **47**, 1755–1777.

——, and R. B. Smith, 1986: Transient dynamics of airflow near a local heat source. *J. Atmos. Sci.*, **43**, 40–49.

——, and H.-Y. Chun, 1991: Effects of diabatic cooling in a shear flow with a critical level. *J. Atmos. Sci.*, **48**, 2476–2491.

Long, R. R., 1953: Some aspects of the flow of stratified fluids. I. A theoretical investigation. *Tellus*, **5**, 42–58.

Moncrieff, M. W., 1978: The dynamical structure of two-dimensional steady convection in constant vertical shear. *Quart. J. Roy. Meteor. Soc.*, **104**, 543–567.

——, 1981: A theory of organized steady convection and its transport properties. *Quart. J. Roy. Meteor. Soc.*, **107**, 29–50.

——, and J. S. A. Green, 1972: The propagation and transfer properties of two-dimensional steady convection in constant vertical shear. *Quart. J. Roy. Meteor. Soc.*, **98**, 336–394.

——, and M. J. Miller, 1976: The dynamics and simulation of tropical squall-lines. *Quart. J. Roy. Meteor. Soc.*, **102**, 373–394.

Peltier, W. R., and T. L. Clark, 1983: Nonlinear mountain waves in two and three spatial dimensions. *Quart. J. Roy. Meteor. Soc.*, **109**, 527–548.

Raymond, D. J., 1986: Prescribed heating of a stratified atmosphere as a model for moist convection. *J. Atmos. Sci.*, **43**, 1101–1111.

Smith, R. B., 1985: On severe downslope winds. *J. Atmos. Sci.*, **42**, 2597–2603.

——, and Y.-L. Lin, 1982: The addition of heat to a stratified airstream with application to the dynamics of orographic rain. *Quart. J. Roy. Meteor. Soc.*, **108**, 353–378.

——, and J. Sun, 1987: Generalized hydraulic solutions pertaining to severe downslope winds. *J. Atmos. Sci.*, **44**, 2934–2939.

Thorpe, A. J., M. J. Miller, and M. W. Moncrieff, 1980: Dynamical model of two-dimensional downdraughts. *Quart. J. Roy. Meteor. Soc.*, **106**, 463–484.